

## MODELING OF SELF-HEATING IN IC INTERCONNECTS AND INVESTIGATION ON THE IMPACT ON INTERMODULATION DISTORTION

---

### 2.1 CONCEPT OF SELF-HEATING

As the frequency of operation increases, especially in the RF and microwave range (MHz - GHz), current that flows through resistive elements in ICs causes collision of charge carriers, resulting in an increase in the temperature of the IC.

The physics of self-heating can be given as follows: when a current at RF frequencies passes through a resistive element, collision of charge carriers occurs that causes a change in the temperature of resistive element. This is independent of ambient temperature and hence, appropriately called “self” heating. This heating then causes a change in resistivity, which then affects the time constants of the model, and hence causes undesired frequency components to appear in the output.

This is an undesired effect because of appearance of undesired frequency components, and self heating effects become more prominent as the devices are scaled down, especially towards 90nm and smaller technologies.

The problem of self heating can be accounted for, by coupling thermal and electrical domains and then developing a comprehensive model.

### 2.2 INTERCONNECTS AND TRANSMISSION LINE MODELS

In today’s VLSI circuits, in order to minimize chip size, we often go for multilayered interconnects, a typical example of which is shown below.

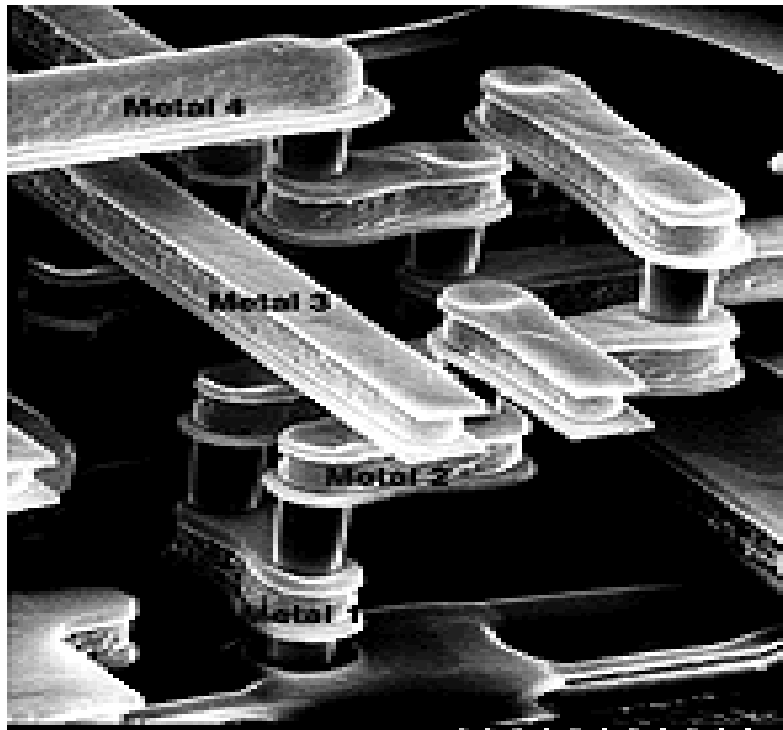


Figure 4 Multilayered interconnect

As seen above, there are various metal layers one above the other, separated with insulators in between. These interconnects can be modeled using standard transmission line models.

The transmission line models used most commonly to represent interconnects are:

1. The coplanar model (within a metal layer)
2. The microstrip model (between two metal layers of different heights).

The model parameters used in this work are as given below:

# MODEL PARAMETERS

- **MICROSTRIP:**

- SUBSTRATE : SiO<sub>2</sub>
- CONDUCTOR: Al
- CONDUCTOR WIDTH: 6 $\mu$ m
- CONDUCTOR THICKNESS: 0.1 $\mu$ m
- SUBSTRATE HEIGHT: 100 $\mu$ m
- LINE LENGTH: 1mm

- **COPLANAR:**

- SUBSTRATE : SiO<sub>2</sub>
- CONDUCTOR: Al
- CONDUCTOR WIDTH: 6 $\mu$ m
- SLOT SPACING: 5 $\mu$ m
- CONDUCTOR THICKNESS: 0.1 $\mu$ m
- SUBSTRATE HEIGHT: 100 $\mu$ m
- LINE LENGTH: 1mm

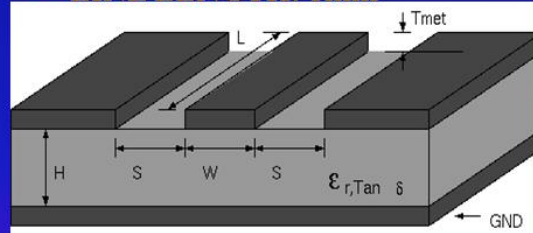
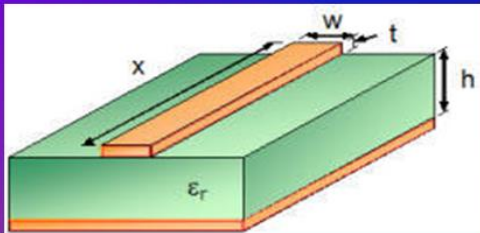


Figure 5 Model parameters

## 2.3 EQUIVALENT CIRCUITS OF TRANSMISSION LINE MODELS

Both coplanar and microstrip models can be modeled using passive RLC (resistor – inductor – capacitor) elements. The values of R, L and C can be found out from the device dimensions using certain relations. These are lossy line models, including the resistive losses. As will be seen later, it is in the resistor that self heating plays a vital role.

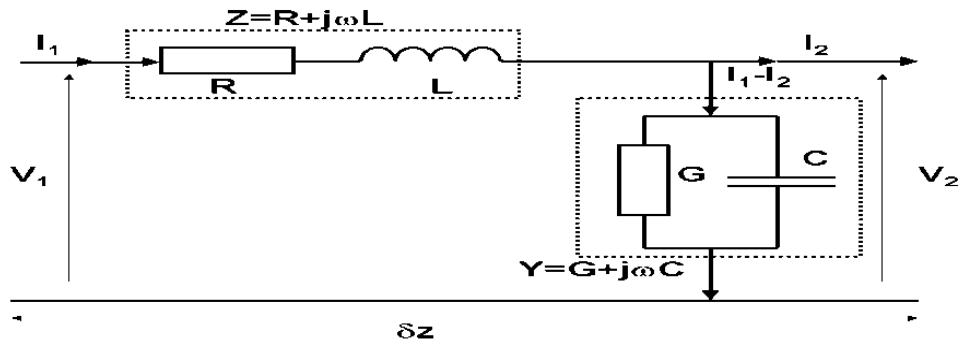


Figure 6 Equivalent circuit

## 2.4 TWO TONE TEST AND INTERMODULATION DISTORTION

Usually, to test for nonlinear effects in line models, we use certain test signals. One such signal that is commonly used is the 2-tone signal which is the sum of 2 sinusoids of different frequencies. This is represented as follows:

$$x(t) = a_1 \cos [f_1 t + u(t)] + a_2 \cos (f_2 t)$$

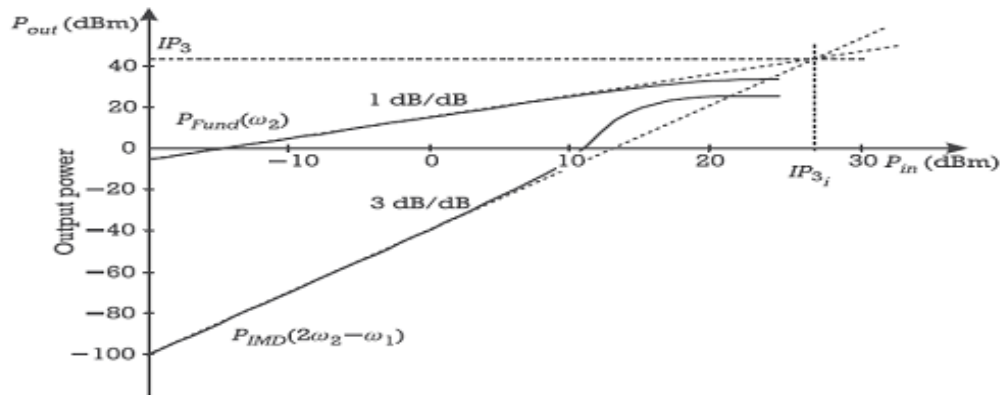
In our model, we used this 2 tone signal with the frequency of separation ranging from tens of Megahertz to tens of Gigahertz. When the 2 tone signal is passed through a nonlinear model a wide range of frequencies, created by the sum and difference of the fundamental frequencies and their harmonics are formed.

Hence if the input tones are  $f_1$  and  $f_2$ , we have  $f_1$ ,  $f_2$ ,  $2f_1$ ,  $2f_2$ ,  $f_1 - f_2$ ,  $f_1 + f_2$ ,  $3f_1$ ,  $3f_2$ ,  $2f_1 - f_2$ ,  $2f_1 + f_2$ ,  $2f_2 - f_1$  and  $2f_2 + f_1$ , (approximated third order). Out of these, all frequencies except  $f_1$ ,  $f_2$ ,  $2f_2 - f_1$ , and  $2f_1 - f_2$  are called “out-of-band” products and can be easily filtered out. The in-band frequencies are  $f_1$ ,  $f_2$ ,  $2f_1 - f_2$ , and  $2f_2 - f_1$ . Out of these  $f_1$  and  $f_2$  are the desired output frequencies. The distortion caused by the remaining frequencies ( $2f_1 - f_2$ , and  $2f_2 - f_1$ ) are called “intermodulation distortion” (IMD)

Hence IMD is the most critical form of distortion as these frequencies can neither be filtered out nor be ignored. As will be seen later, it is the Third Order IMD (IMD3) i.e  $2f_2-f_1$  and  $2f_1-f_2$  that cause much of the problem with regards to self heating.

## 2.5 CHARACTERIZATION AND MEASUREMENT OF IMD3

The 2 means of characterizing IMD3 are intercept point (IP3) and intermodulation ratio (IMR). The means of determining them is as shown.



Output fundamental power per tone and distortion power in one IMD sideband for an equal amplitude two-tone excitation.

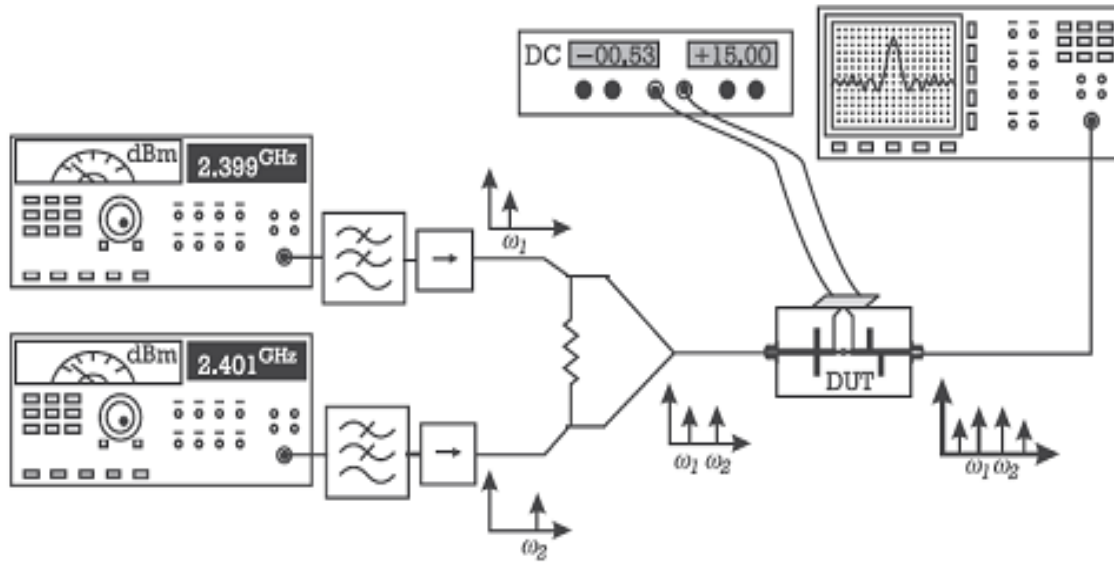
Figure 7 Computation of third order intercept point

Here output power is measured as a function of input power, and the intersection of the extrapolated  $P_{in}$  and  $P_{IMD}$  gives  $IP_3$ .

$$IMR \equiv \frac{P_{fund}}{P_{IMD}} = \frac{P(\omega_1)}{P(2\omega_1 - \omega_2)} = \frac{P(\omega_2)}{P(2\omega_2 - \omega_1)}$$

Figure 8 Computation of IMR

Shown below is the most commonly used setup for measuring IMD3.



Most commonly used two-tone test measurement setup.

Figure 9 Two tone measurement setup

## 2.6 MULTISIM IMPLEMENTATIONS OF LINEAR AND NONLINEAR TRANSMISSION LINES

To better understand the effects of IMD due to line nonlinearity, we simulated first a linear transmission line (microstrip) based on the equivalent circuit in MultiSim and then observed the Waveforms and Fourier Spectrum. The results are as shown below:

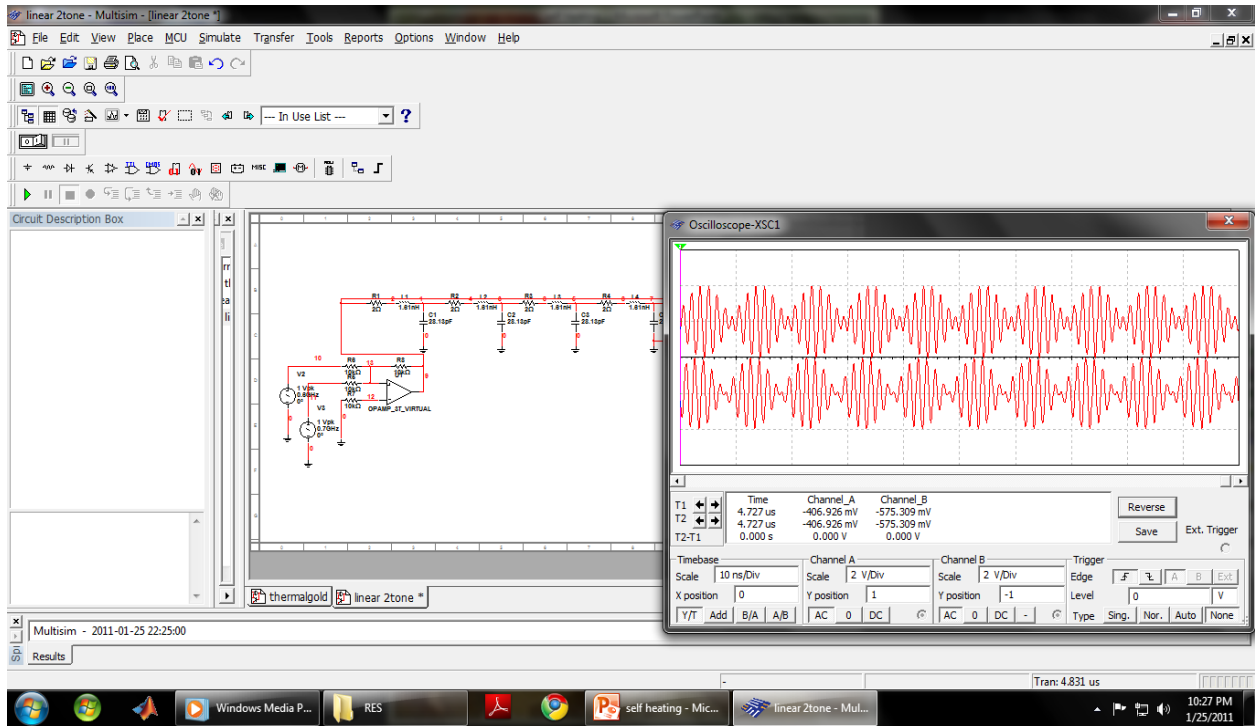


Figure 10 Linear Transmission line

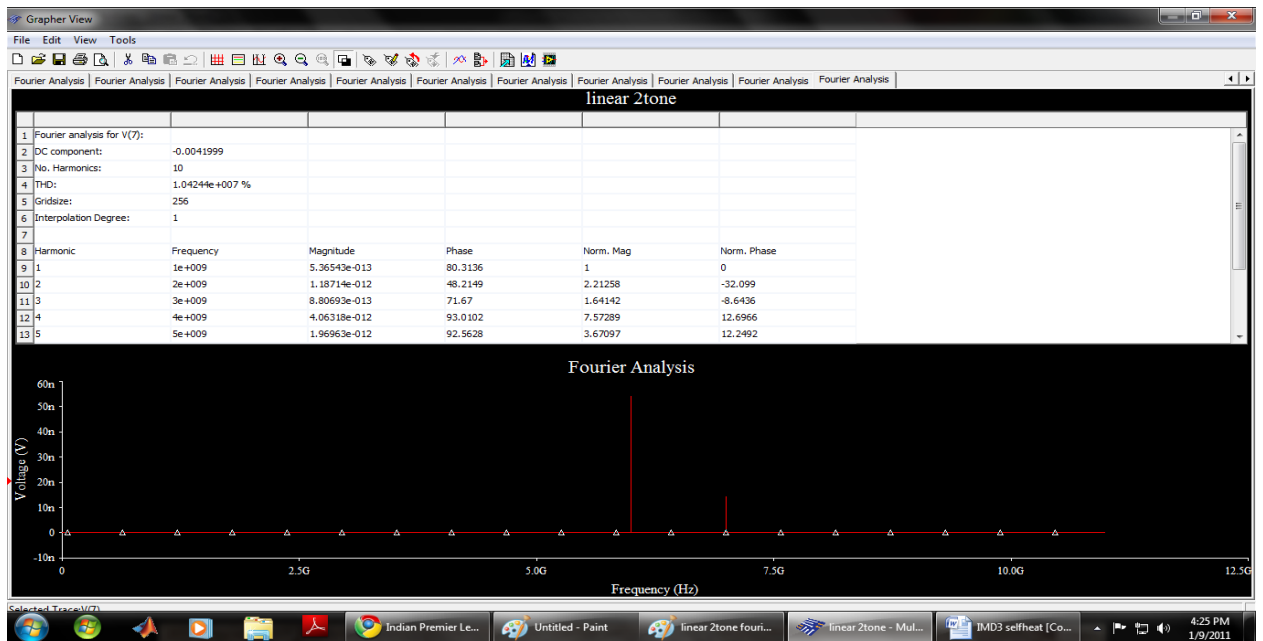


Figure 11 Output Fourier Spectrum

Next we repeated the simulations, but this time with a nonlinear transmission line obtained by replacing the capacitors with the varactors.

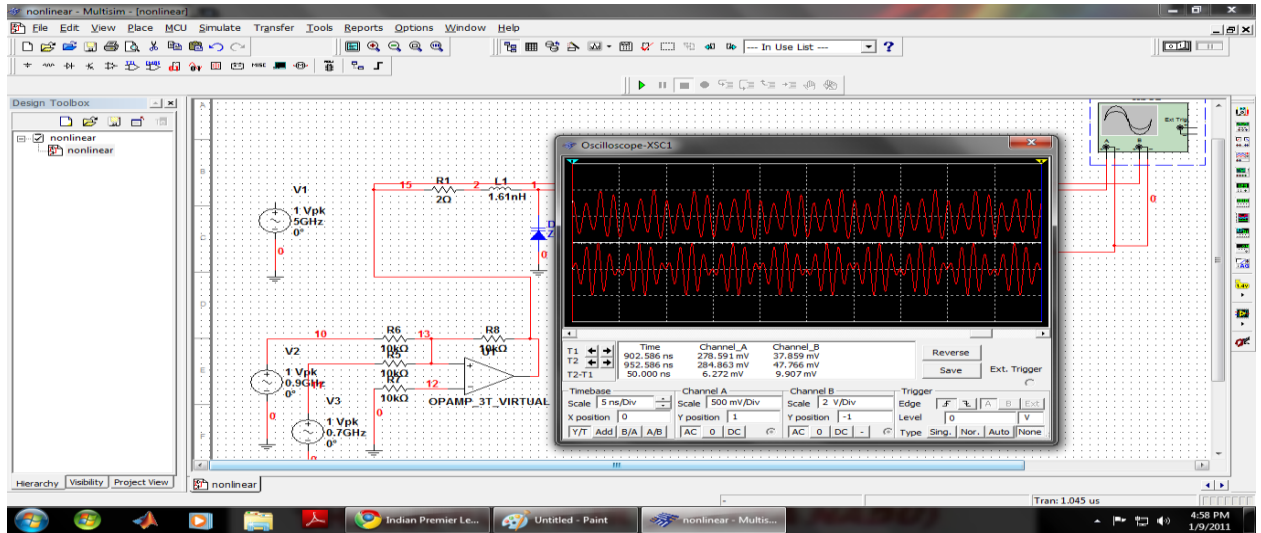


Figure 12 Nonlinear transmission line waveform

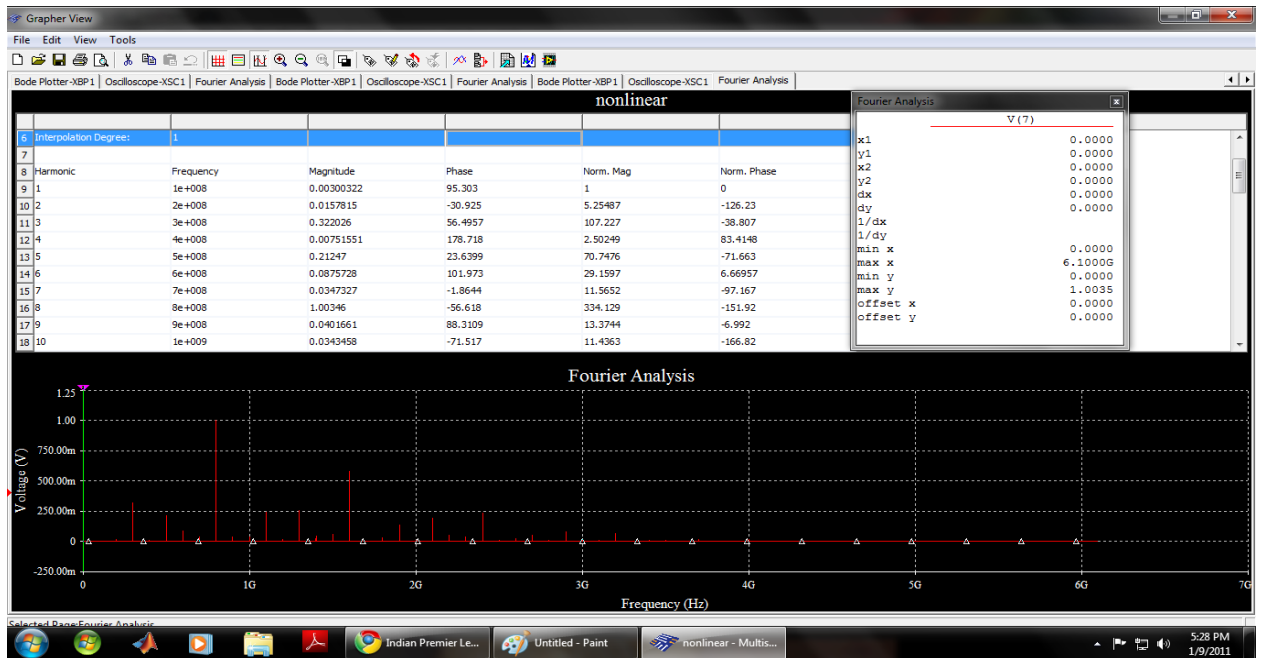


Figure 13 Output spectrum

As can be seen the nonlinear transmission line shows a lot of other components other than the input frequencies, and these components contain both inband and out-of band distortion components. Thus the intermodulation distortion was effectively understood using the equivalent circuits.

## 2.7 ELECTRO-THERMAL THEORY OF SELF-HEATING

Self – heating causes Intermodulation distortion and this is called ET-PIM (electro- thermal passive intermodulation distortion). This is explained in the paper by Wilkerson et al. and is outlined briefly here:

***THE COLLISION OF CHARGE CARRIERS IN A RESISTIVE ELEMENT CAUSES CHANGE IN TEMPERATURE AND THIS CHANGE IS PERIODIC, WITH A BASEBAND RANGE. NOW, WHEN A 2 TONE INPUT SIGNAL IS GIVEN AS INPUT, THE POWER SPECTRUM CONSISTS OF THE SUM ( $F_1+F_2$ ) AND THE DIFFERENCE ( $F_1-F_2$ , ALSO CALLED ENVELOPE OR BEAT FREQUENCY). IF THE BEAT FREQUENCY HAPPENS TO FALL IN THIS BASEBAND RANGE, THE THERMAL EFFECTS BECOME PROMINENT, PERIODICALLY VARYING THE RESISTANCE. IN EFFECT, THIS CREATES A PASSIVE MIXER PRODUCING INTERMODULATION DISTORTION THROUGH UPCONVERSION OF THE ENVELOPE FREQUENCIES AT BASEBAND TO RF FREQUENCIES. THESE FREQUENCIES ARE NOTHING BUT THOSE ARISING IN IMD3 (THIRD ORDER INTERMODULATION DISTORTION).***

This is clearly illustrated in the following diagram:

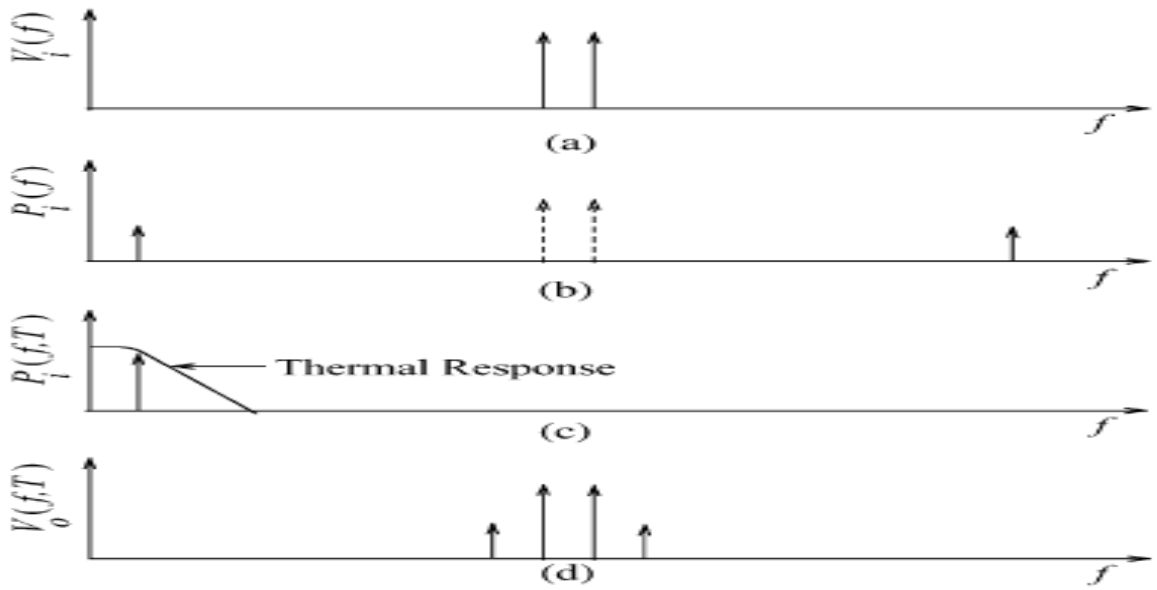


Fig. 1. Passive mixing process inherent in coupled electrical and thermal systems with: (a) input spectrum of voltages  $V_i(f)$  resulting from two-tone excitation, (b) input power spectrum  $P_i(f)$  resulting from a two-tone excitation, (c) component of the input power spectrum  $P_i(f, T)$  at baseband able to interact with the thermal response, and (d) output spectrum of voltages  $V_o(f, T)$  after electro-thermal mixing has occurred.

Figure 14 Electro Thermal Theory of Self Heating

Mathematically the expressions denoting the process are as follows:

- WE FIRST START WITH THE THERMO-RESISTANCE EQUATION GIVEN AS:
 
$$\rho_e(T) = \rho_{e0}(1 + \alpha T + \beta T^2 + \dots)$$
- HEAT GENERATED THROUGH SELF HEATING CAN BE GIVEN AS FOLLOWS:
 
$$Q = J^2 \rho_e$$
- NEXT THE HEAT CONDUCTION EQUATION IS GIVEN BY:
 
$$\nabla \cdot \left( \frac{\nabla T}{R_{th}} \right) - \rho_e c_v \frac{\partial T}{\partial t} = Q$$
- THUS THE DIFFERENTIAL EQUATION EXPRESSING THE NONLINEARITY IS:
 
$$\nabla \cdot \left( \frac{\nabla T}{R_{th}} \right) - C_v \frac{\partial T}{\partial t} = J^2 \rho_{e0}(1 + \alpha T + \beta T^2 + \dots)$$
- USING EVOLUTION AND FRACTIONAL CALCULUS WE GET THE EQUATION OF TEMPERATURE AS:
 
$$T = A e^{-kx} \cos(\omega t - kx)$$

$$k = (\omega/2\kappa)^{1/2}$$

Figure 15 Expressions of self heating

### 2.8 COMPACT MODELING OF SELF HEATING

The equations and resulting changes can be given as an equivalent circuit which acts as a replacement of the resistor in the transmission line models.

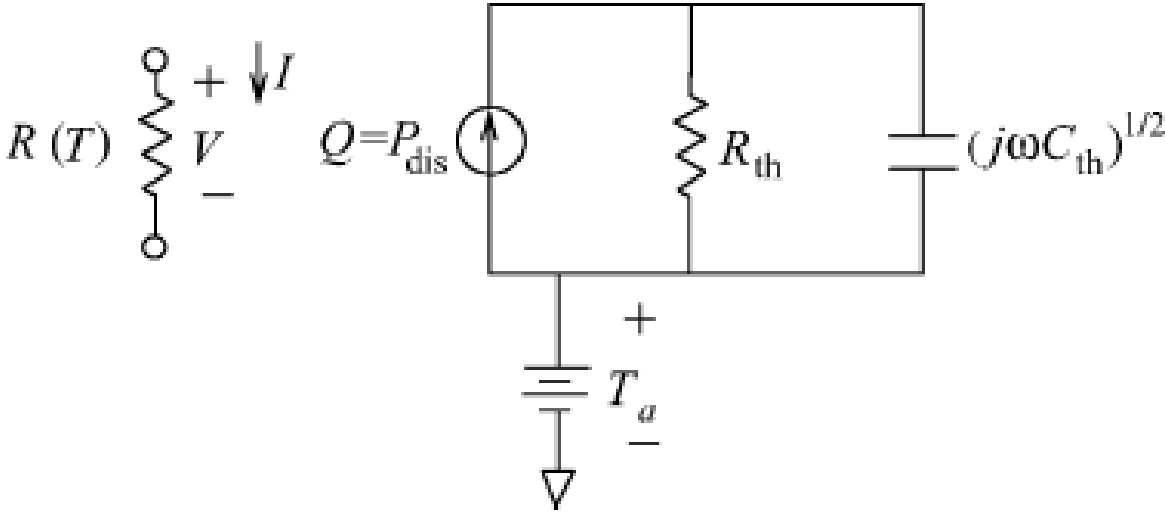


Figure 16 Equivalent circuit of resistor

Here, Q Is The Input To The Model And This Is The Power Dissipated Through The Resistor, Ta Represents Ambient Temperature. The expressions for the Rth and Cth are as follows:

**THERMAL RESISTANCE IS GIVEN BY**

$$\kappa = (R_{th}C_v)^{-1}, \quad R_{th} = \frac{\Delta T}{P} = \frac{\Delta T}{I^2 R}$$

**AND THE THERMAL CAPACITANCE CAN BE CALCULATED USING THE FOLLOWING.**

$$C_v = \left( \frac{\partial Q}{\partial T} \right)_v = T \left( \frac{\partial S}{\partial T} \right)_v = c_v \rho_d V. \quad C_{th} = C_v R_{th}$$

**HERE  $c_v$  IS THERMAL CAPACITY,  $\rho_d$  IS DENSITY, V IS VOLUME, AND  $\kappa$  IS THERMAL DIFFUSIVITY**

Figure 17 Rth and Cth for self heating equivalent circuit

## 2.9 TRANSMISSION LINE MODELS INCLUDING SELFHEATING EFFECTS

Next, we implement Transmission line models including the effects of self heating. To start with, we implement Microstrip made of Aluminium SOI as a model including self heating effects, and set the 2 tones at 600MHz and 700MHz. The results are as follows:

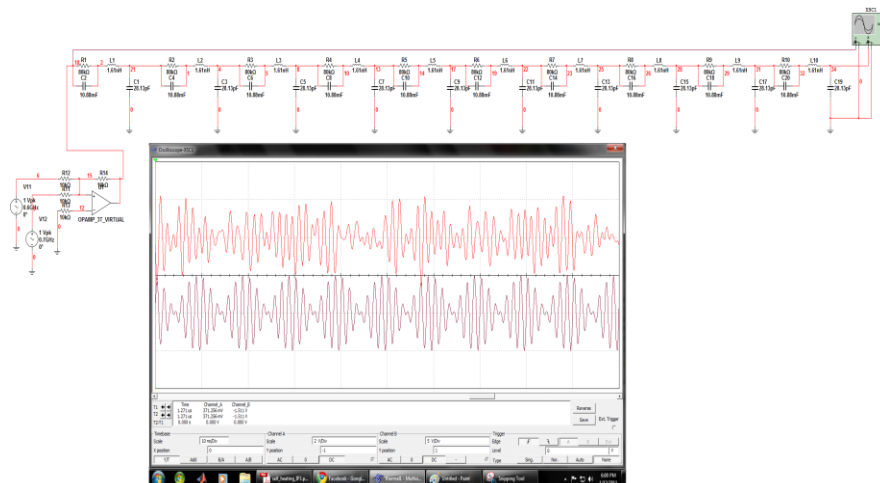


Figure 18 Aluminium microstrip waveforms

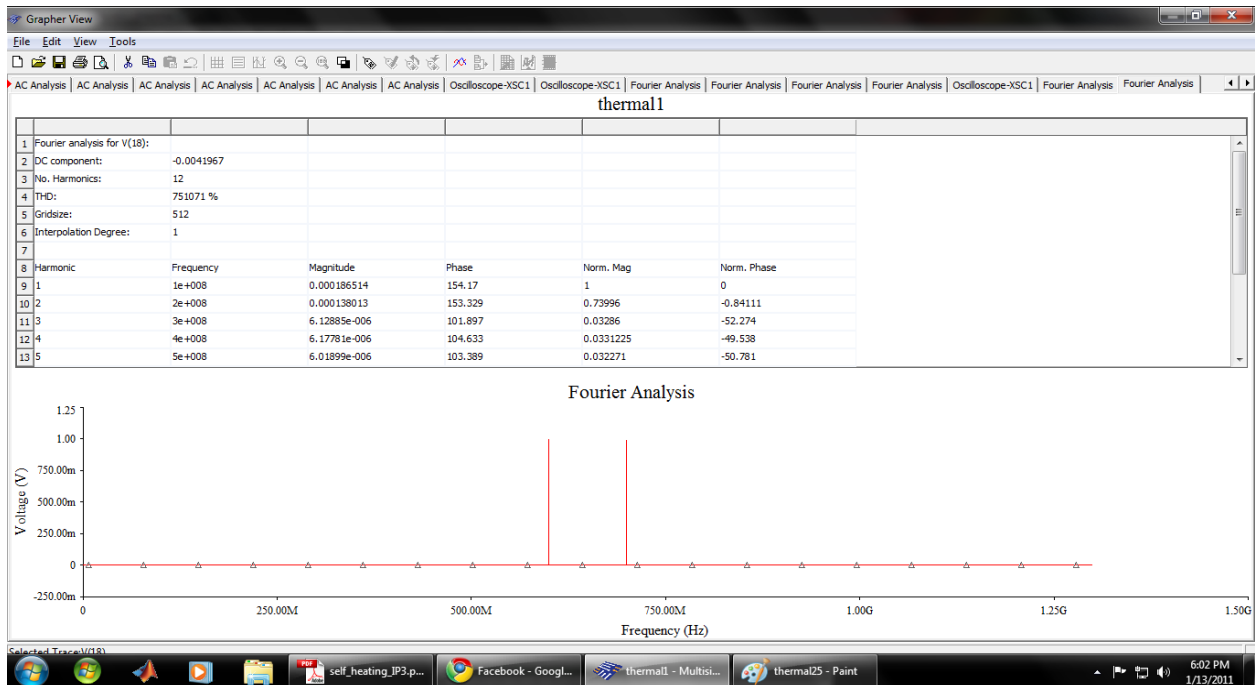


Figure 19 Input Fourier Spectrum

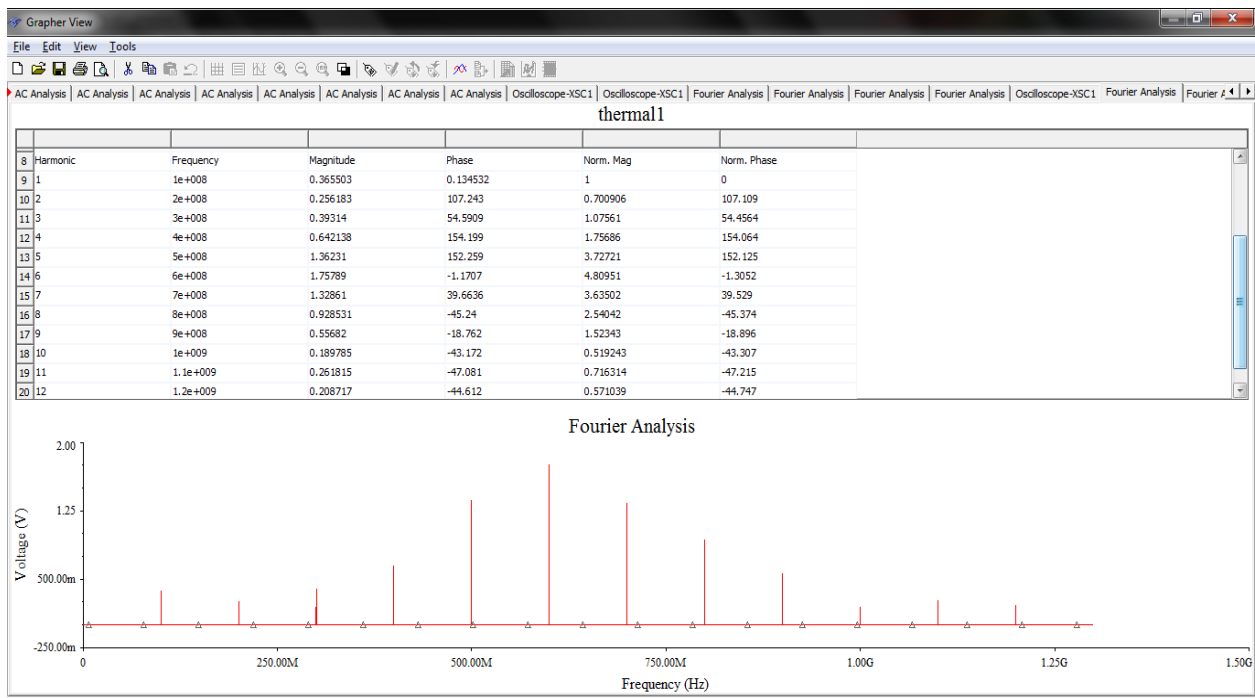


Figure 20 Output spectrum

As we can see in Fourier analysis of output, there is significant amplitude of the desired components, 600 and 700 MHz (the 2 tones). In addition we have components at 800 and 500 MHz which are the IMD3 frequencies. There are components in other frequencies as well. For example, 400 and 900 MHz But these are far apart from the desired frequency (600 and 700 MHz) and hence can be easily filtered out using appropriate band pass filters.

Next we repeat the same but with the 2 tones at 300 and 400MHz. The results are as follows:

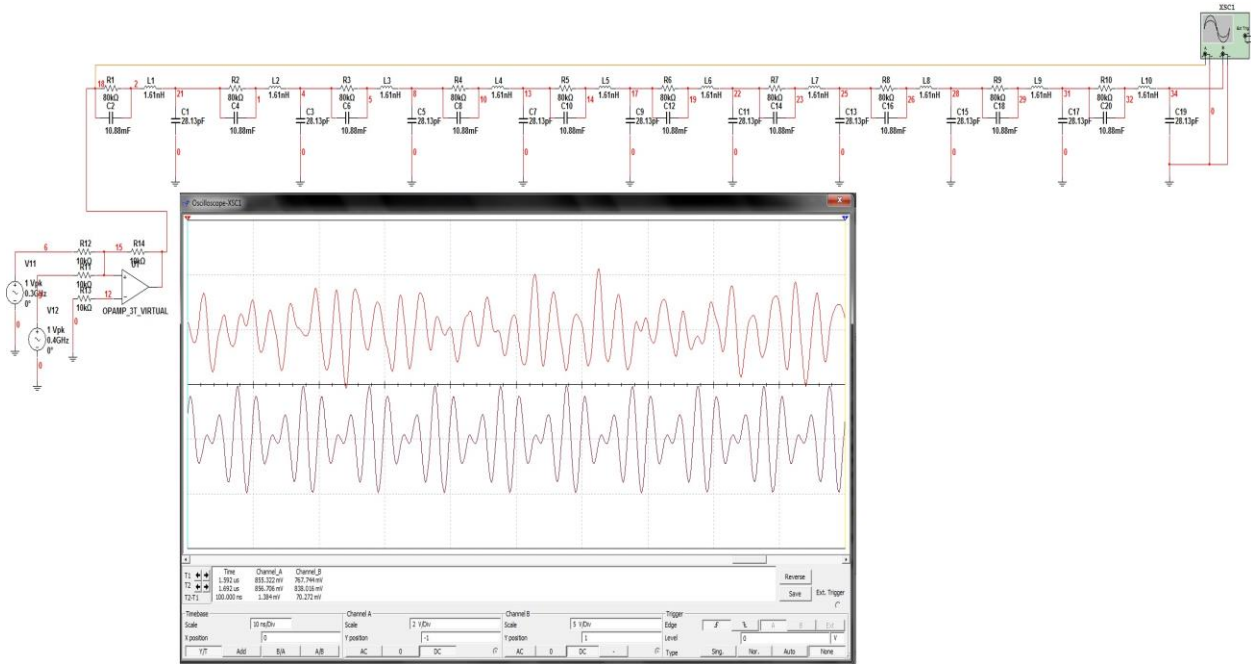


Figure 21 Aluminium Microstrip Waveforms

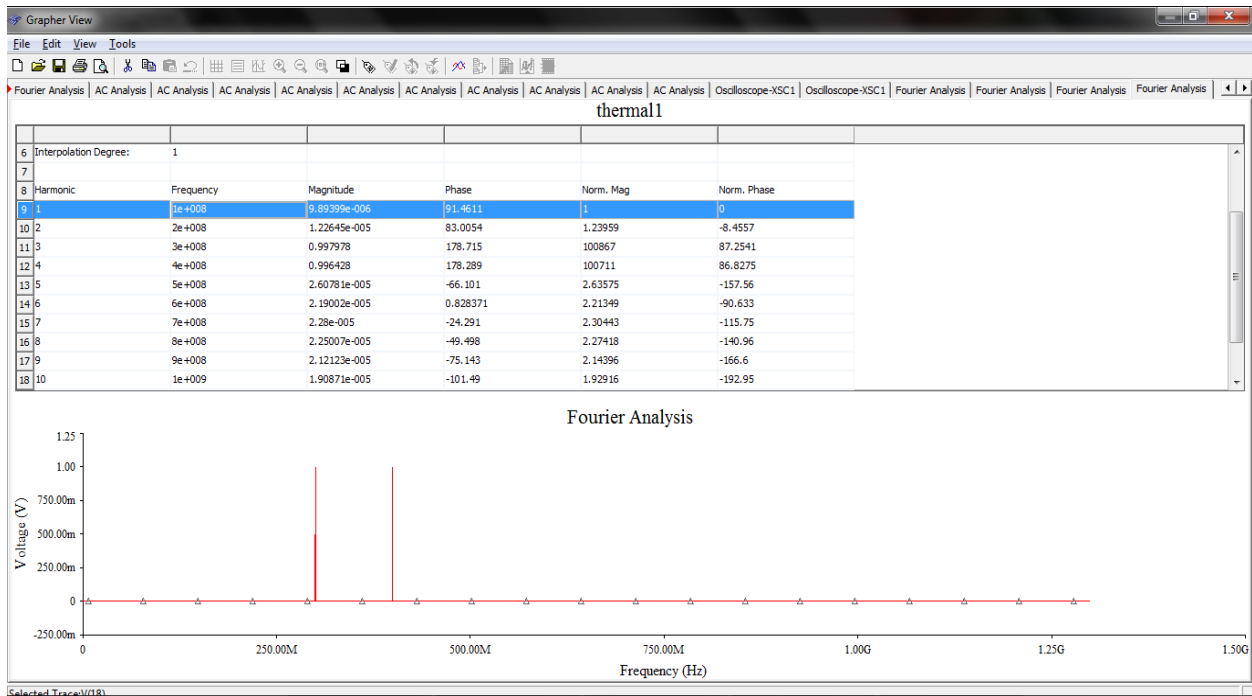


Figure 22 Input spectrum

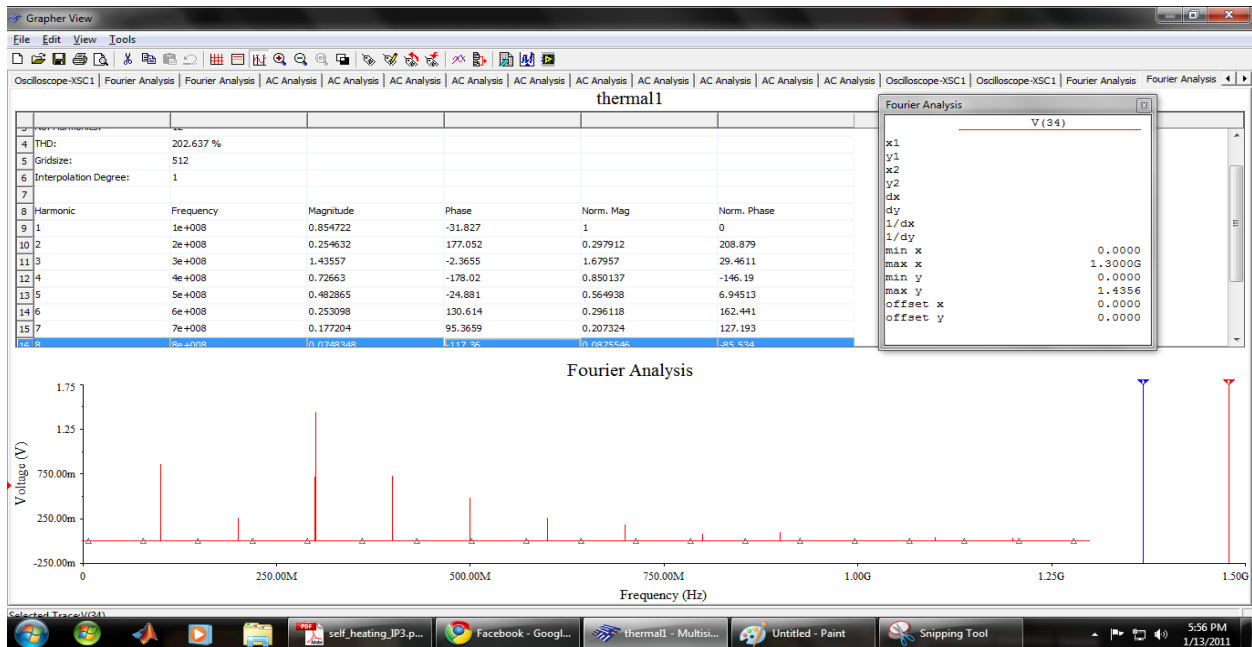


Figure 23 Output spectrum

As we can see in Fourier analysis of output, there is significant amplitude of the desired components, 300 and 400 MHz (the 2 tones). In addition we have components at 500 and 200 MHz which are the IMD3 frequencies. There are components in other frequencies as well. For example, 100, 600, 700 MHz But these are far apart from the desired frequency (300 and 400 MHz) and hence can be easily filtered out using appropriate band pass filters.

From the equations regarding self-heating that were described earlier, we could observe that resistance changes as a function of temperature which in turn varies with time. So we can conclude that resistance varies with temperature. The plot of resistance (ohm) as a function of time (us) for a frequency separation of 999MHz is shown below:

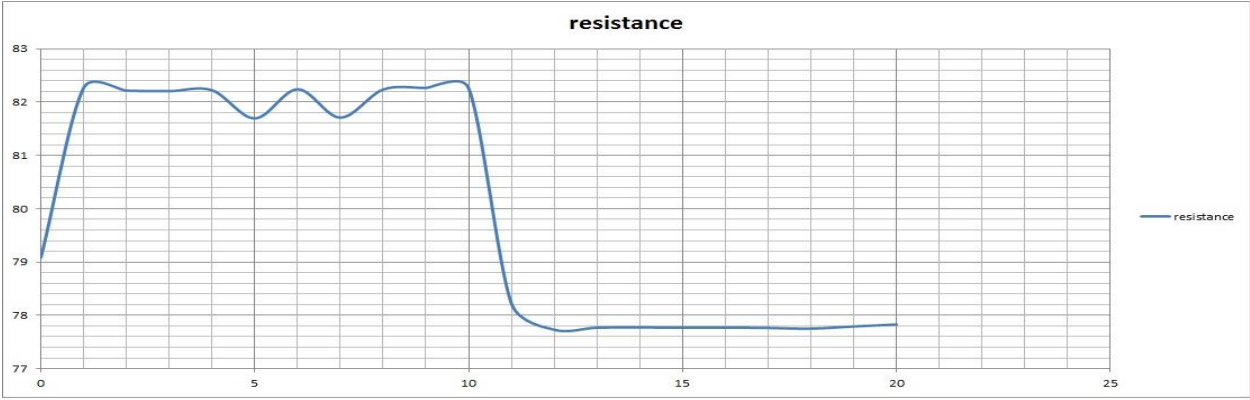


Figure 24 Resistance variations

## 2.10 VERIFICATION OF THE COMPACT MODEL

The compact model has to be verified and checked for consistency. For this we considered a similar model was devised by Eduard Rocas et al. Mentioned in their paper titled “third order intermodulation distortion due to self-heating in gold coplanar waveguides” and they had simulated the model and also verified the results experimentally. Hence in order to verify our model, we tried to reproduce the results by simulating a gold coplanar transmission line of the dimensions specified by them. The model parameters used by them are as follows:

# MODEL PARAMETERS

- **COPLANAR:**
- **SUBSTRATE :** Sapphire
- **CONDUCTOR:** Gold
- **CONDUCTOR WIDTH:** 30 $\mu$ m
- **SLOT SPACING:** 15 $\mu$ m
- **CONDUCTOR THICKNESS:** 480nm
- **SUBSTRATE HEIGHT:** 200 $\mu$ m
- **LINE LENGTH:** 9.933mm

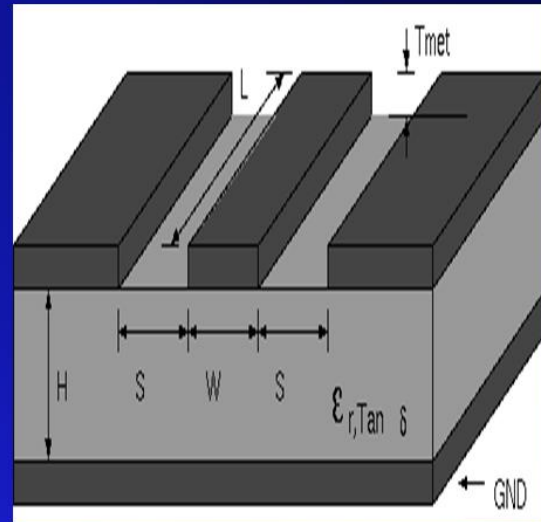


Figure 25 Model parameters of Gold Coplanar Waveguide

The results are as follows:

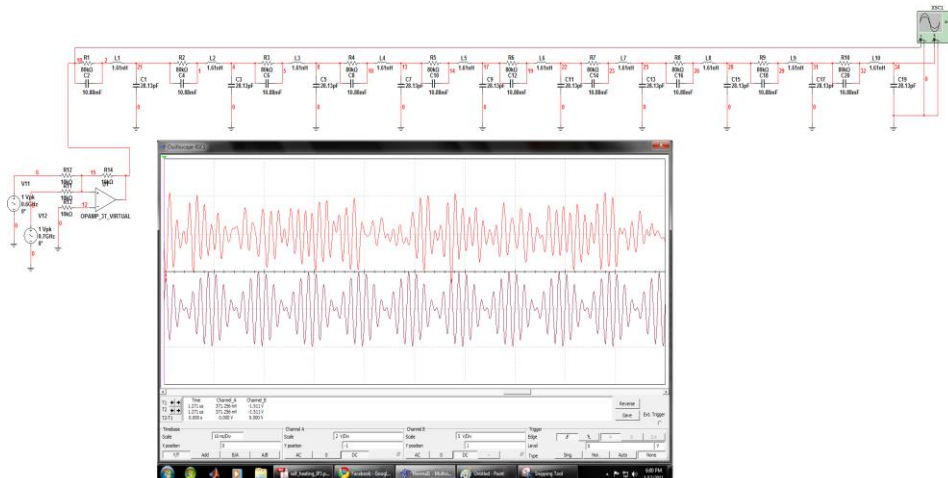


Figure 26 Waveforms for 700 and 800 MHz

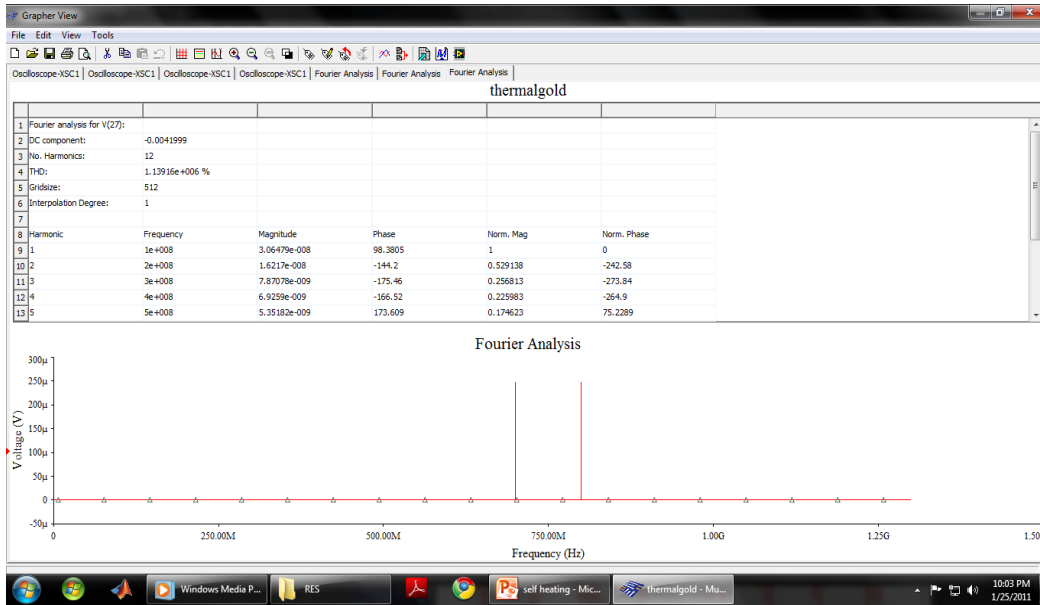


Figure 27 Input spectrum

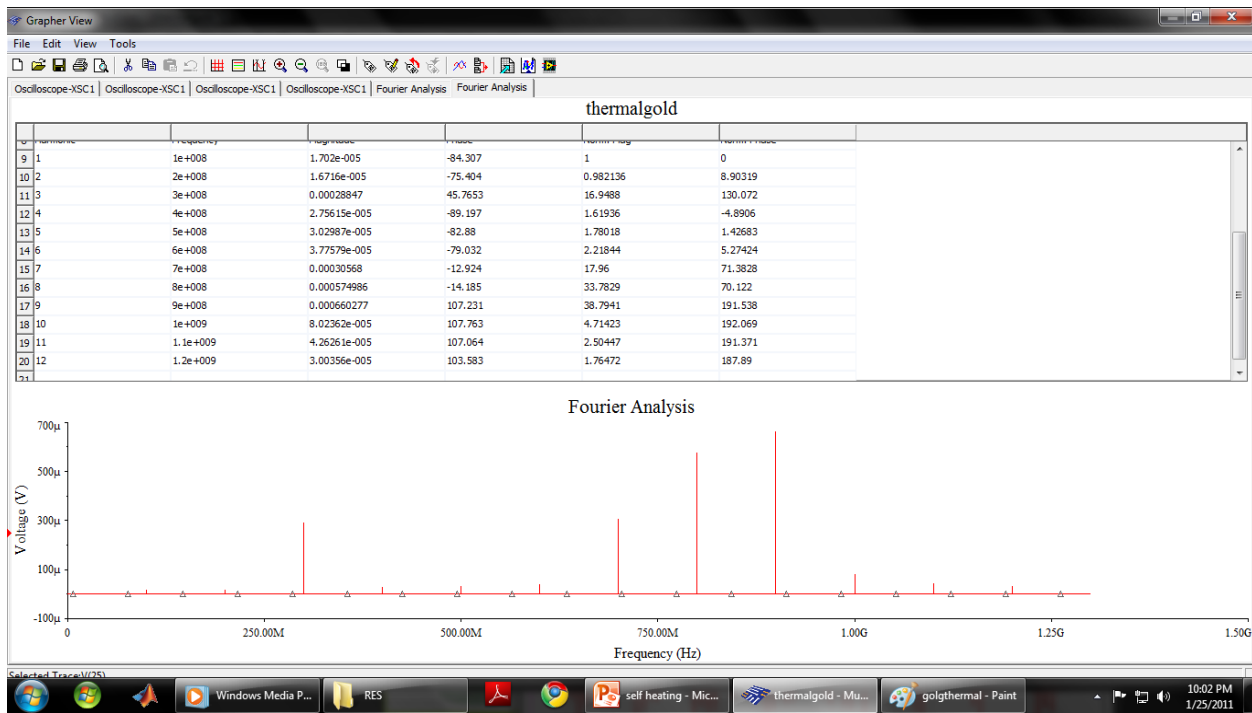


Figure 28 Output spectrum

As we can see in Fourier analysis of output, there is significant amplitude of the desired components, 700 and 800 MHz (the 2 tones). In addition we have components at 600 and 900

MHz which are the IMD3 frequencies. There are components in other frequencies as well. For example, 300, 1000, and 1100 MHz But these are far apart from the desired frequency (700 and 800 MHz) and hence can be easily filtered out using appropriate band pass filters.

Shown below is the frequency separation (MHz) vs. IMD3 (dBm) of the simulated gold CPW model, shown alongside the corresponding curve obtained by Eduard Rocas et al (denoted as A-CPW).

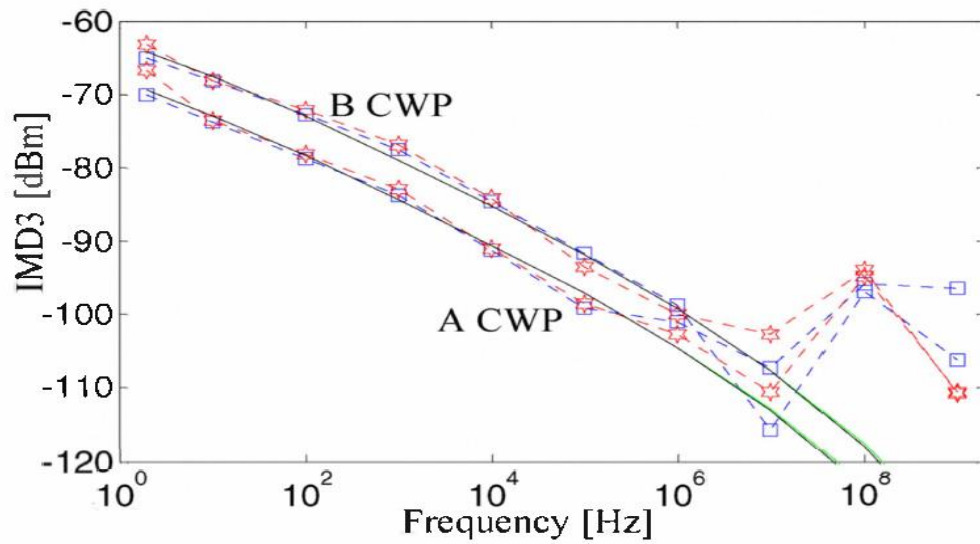


Figure 29 Curves of Eduard

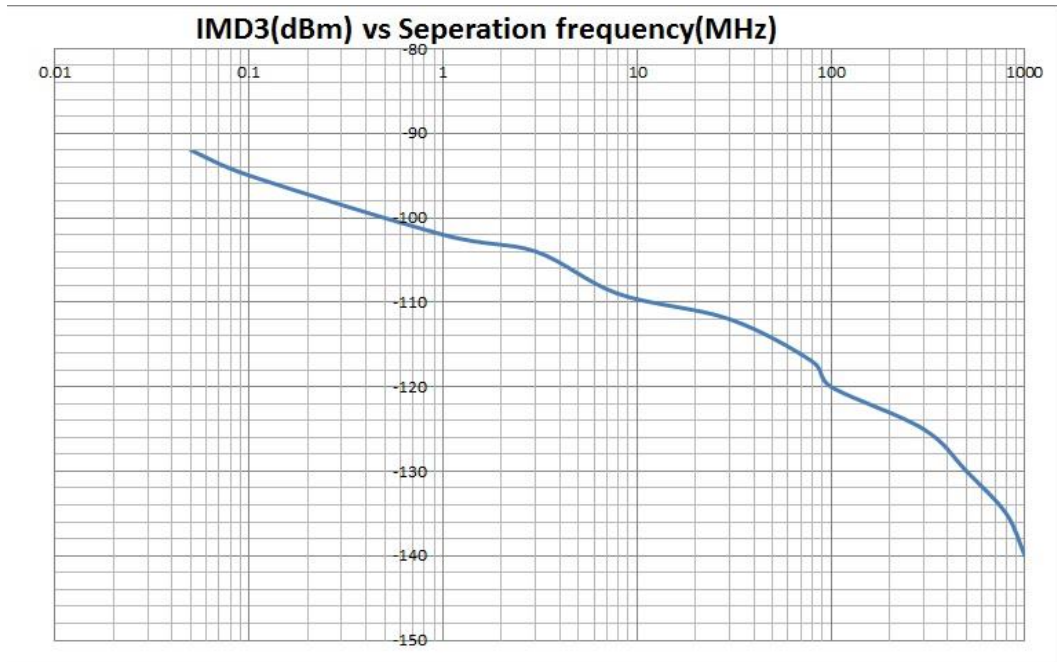


Figure 30 Curves for our model

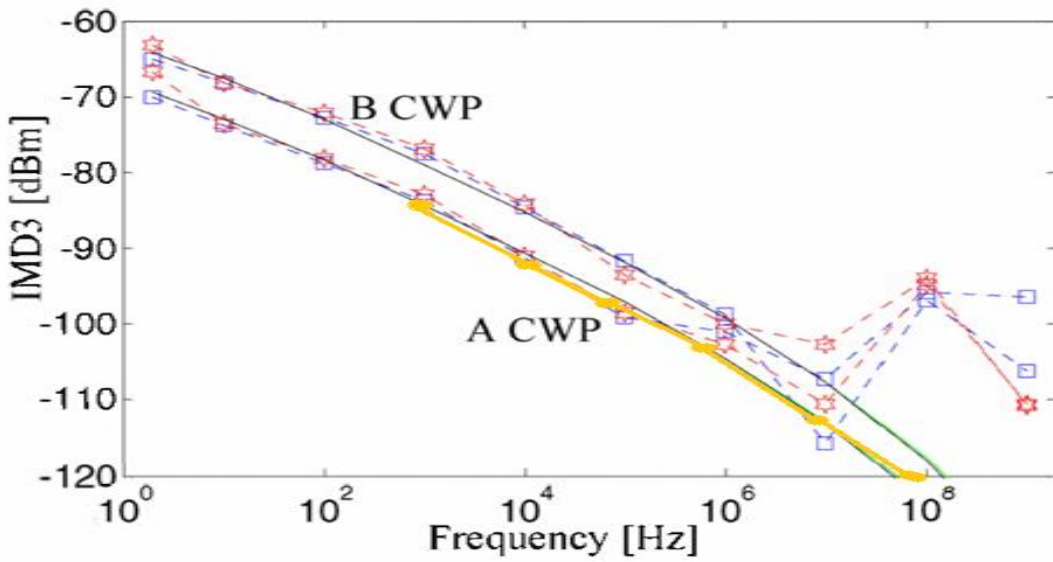


Figure 31 Curves overlaid

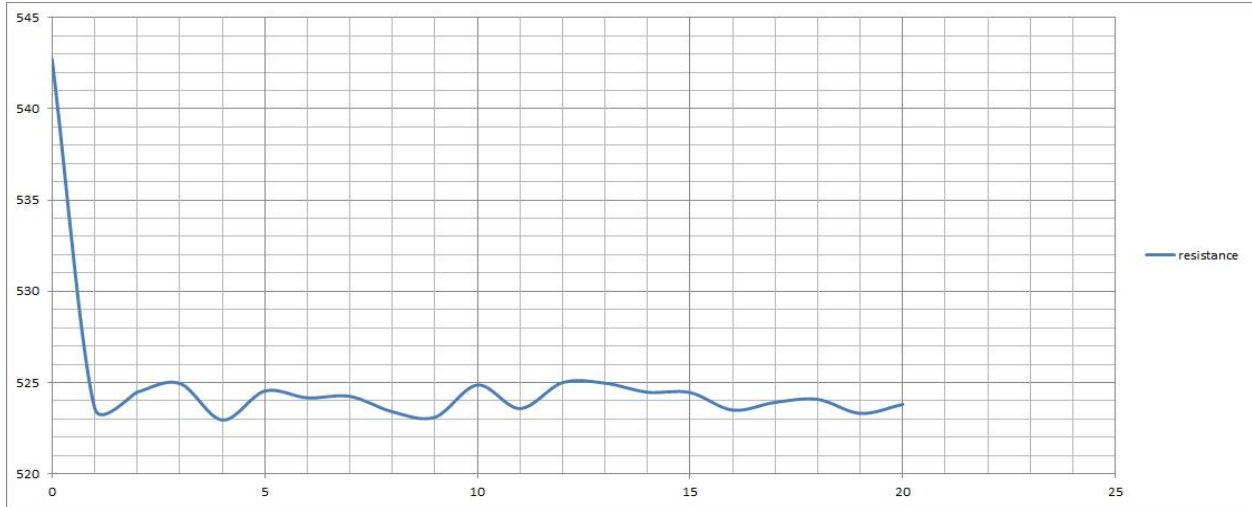


Figure 32 Resistance variations

Thus the above curves assert without doubts the validity and accuracy of the compact model, thus making it as good as measuring the values in the lab and asserting it.

## 2.11 COMPACT MODELING OF BEOL INTERCONNECTS

**Back-end-of-line (BEOL)** denotes the second portion of IC fabrication where the individual devices (transistors, capacitors, resistors, etc.) get interconnected with wiring on the wafer. BEOL generally begins when the first layer of metal is deposited on the wafer. It includes contacts, insulating layers (dielectrics), metal levels, and bonding sites for chip-to-package connections.

The next step is to model the self heating in back end of line (BEOL) interconnects. These are usually made of tantalum which has a negative temperature coefficient of resistance. Thus beol can be modeled as microstrip with the same geometry given earlier but with the conductor replaced by tantalum. The results will now be shown.

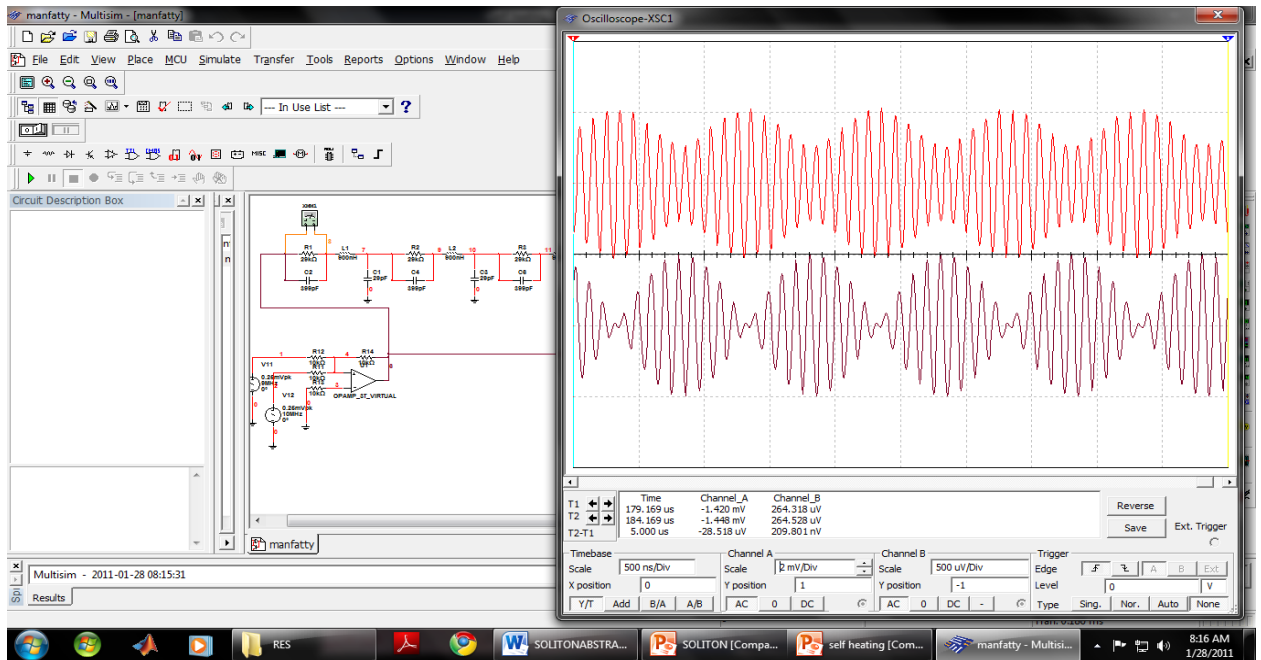


Figure 33 Waveforms of tantalum at 300 and 400 MHz

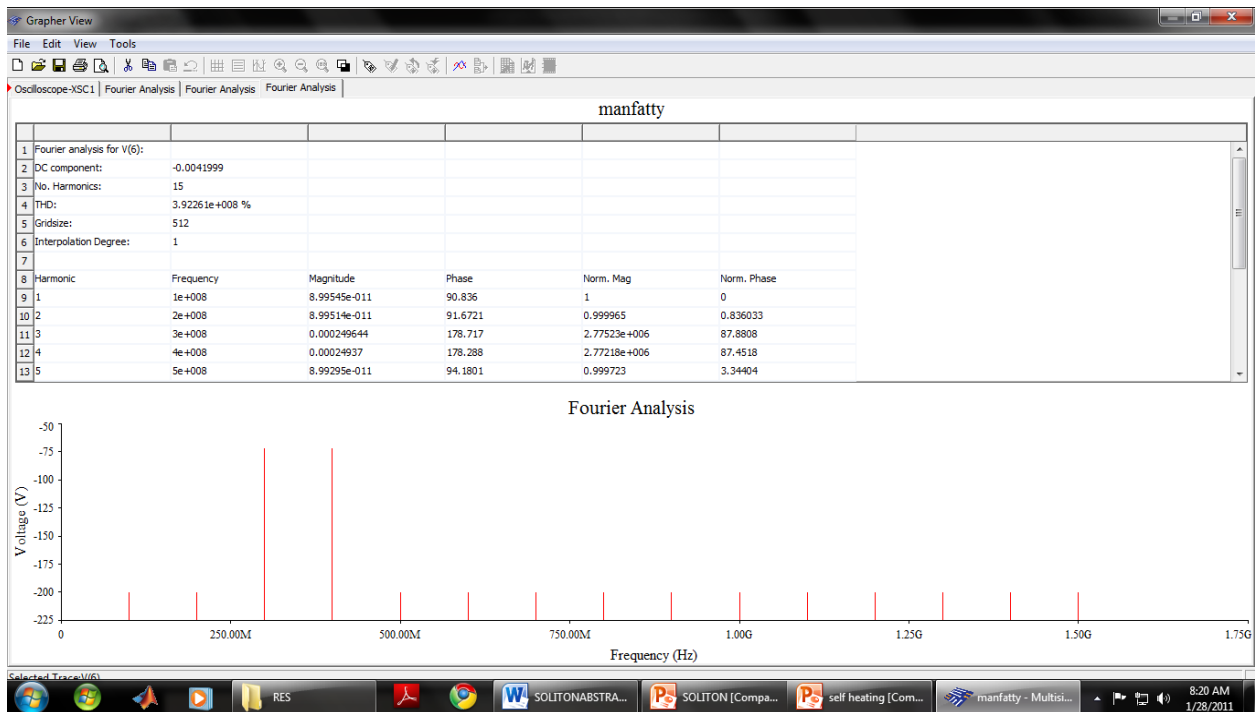


Figure 34 Input spectrum

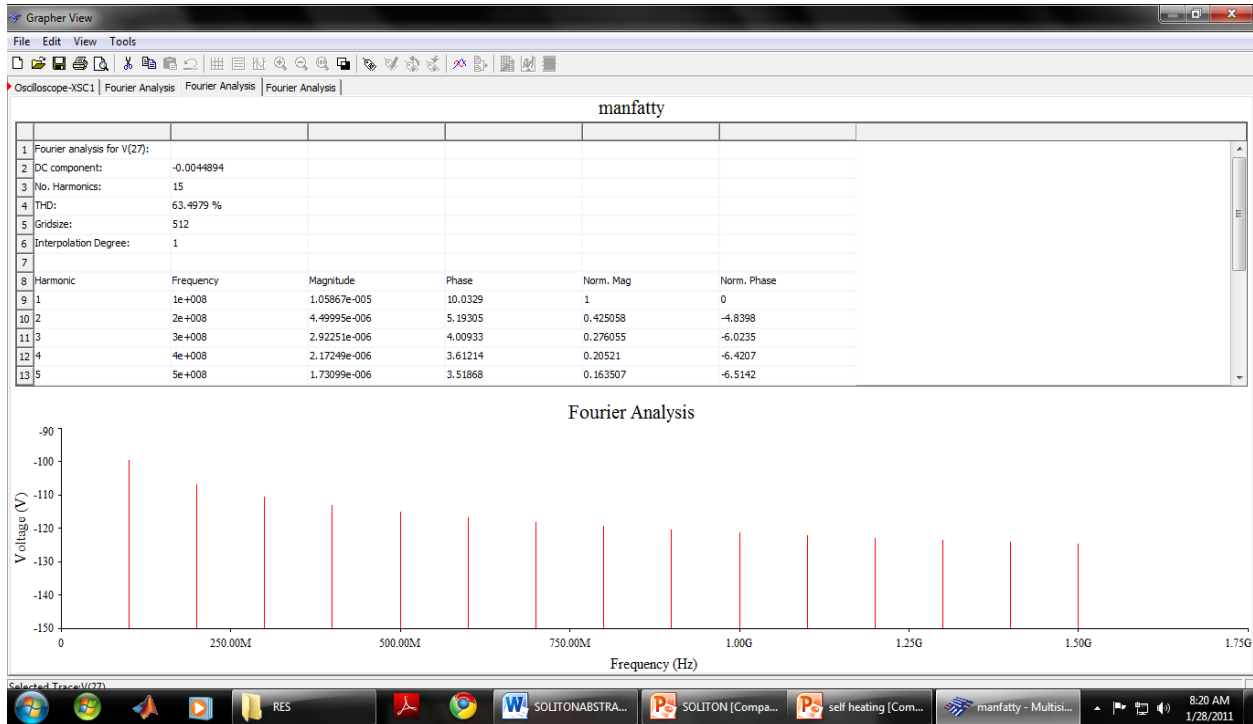


Figure 35 Output spectrum

## 2.12 IMPACT OF SELF HEATING ON INTERMODULATION DISTORTION

As the MultiSim comprehensive model is now validated with the verification of results with gold coplanar waveguide, the next step is to simulate the self heating effects observed in real time in back end of line interconnects., where the material is either aluminium or tantalum and substrate is SiO<sub>2</sub> (SOI technology). Such self heating depends on a number of factors as follows:

1. Whether the model is coplanar strip / microstrip
2. Whether the transmission line is linear or nonlinear (varactor induced nonlinearity)
3. Whether the conductor is aluminium / tantalum.
4. Whether self heating is included or not.

This gives a total of 16 combinations, all of which are simulated with the dimensions specified earlier, and a graph of IMD3 power (dBm) vs. separation frequency ( $\omega_2 - \omega_1$ ) is overlaid and plotted as follows.

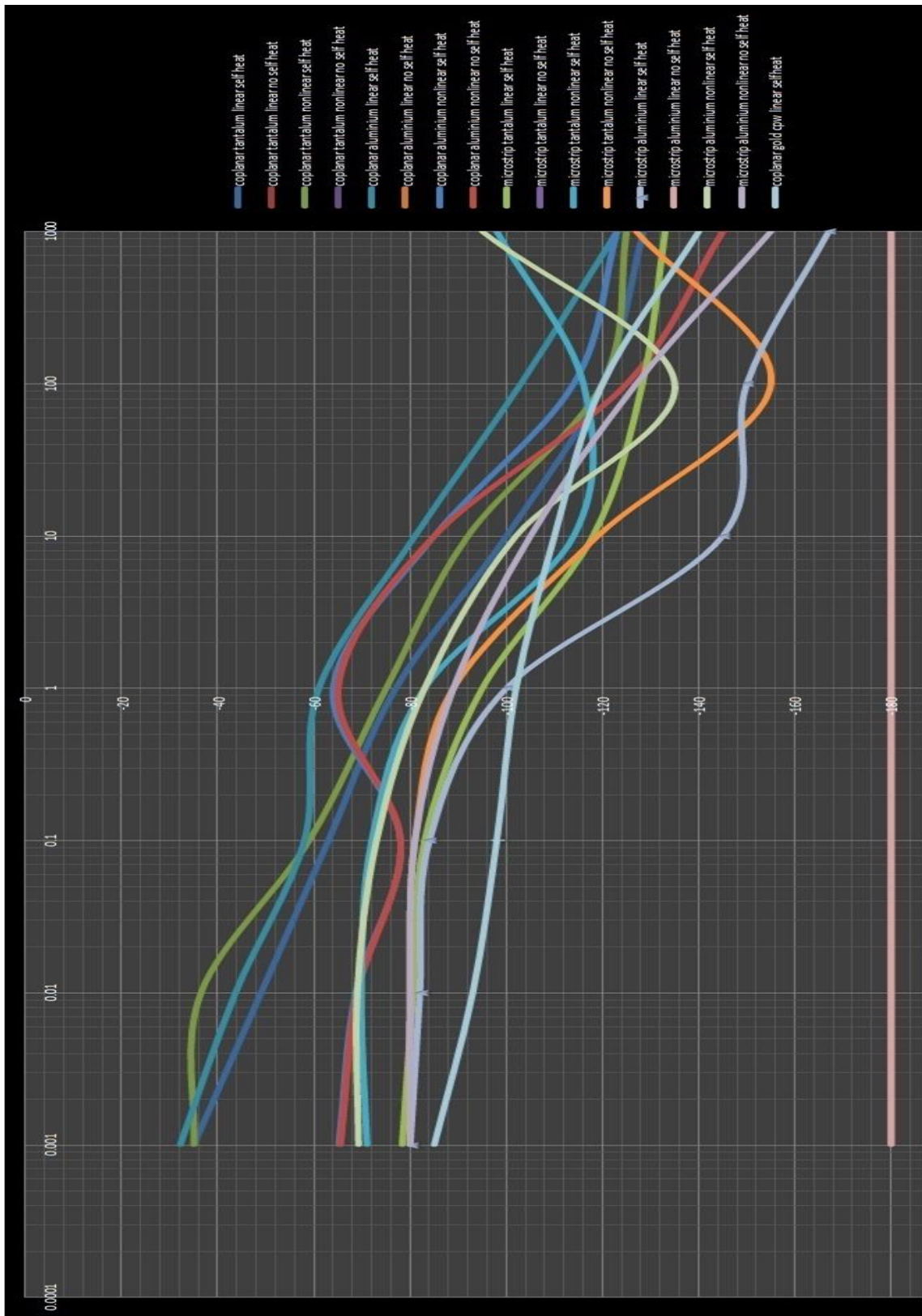


Figure 36 IMD3 vs. frequency separation for 16 cases

FREQUENCY OF SEPERATION (MHz)	IMD3 magnitude in dBm																	
	coplanar tantalum linear self heat		coplanar coplanar tantalum nonlinear self heat		coplanar aluminium linear self heat		coplanar aluminium aluminium nonlinear self heat		microstrip tantalum linear self heat		microstrip tantalum tantalum nonlinear self heat		microstrip aluminium linear self heat		microstrip aluminium aluminium nonlinear self heat		coplanar gold cpw linear self heat	
	linear	linear	nonlinear	nonlinear	linear	linear	nonlinear	nonlinear	linear	linear	nonlinear	nonlinear	linear	linear	nonlinear	nonlinear	linear	linear
	self heat	no self heat	self heat	no self heat	self heat	no self heat	self heat	no self heat	self heat	no self heat	self heat	no self heat	self heat	no self heat	self heat	no self heat	self heat	no self heat
0.001	-35	-180	-35	-65.5	-32.1667	-180	-65.1667	-65.5	-78.36	-180	-71	-80	-80	-180	-69.25	-80	-85	-85
0.01	-49	-180	-36.5	-69	-43.6667	-180	-68.6667	-69	-80.59	-180	-69.85	-80	-82	-180	-69	-80	-93	-93
0.1	-63	-180	-59	-78	-58	-180	-78	-78	-83	-180	-72	-81	-84	-180	-73	-81	-98	-98
1	-77	-180	-75	-65	-61	-180	-64	-65	-95	-180	-83	-89	-100	-180	-83	-89	-102	-102
10	-100	-180	-92	-85	-81	-180	-85	-85	-118	-180	-114	-119	-145	-180	-102	-105	-110	-110
100	-120	-180	-120	-125	-103	-180	-114	-125	-128.29	-180	-116	-155	-150	-180	-135	-127	-120	-120
1000	-128.5	-180	-125	-145	-123	-180	-123	-145	-133	-180	-98	-127	-167	-180	-95	-155	-140	-140

Figure 37 Tabulated values for all 16 cases

To understand the curves better we isolate 3 cases, involving aluminium microstrip and plot them as follows:

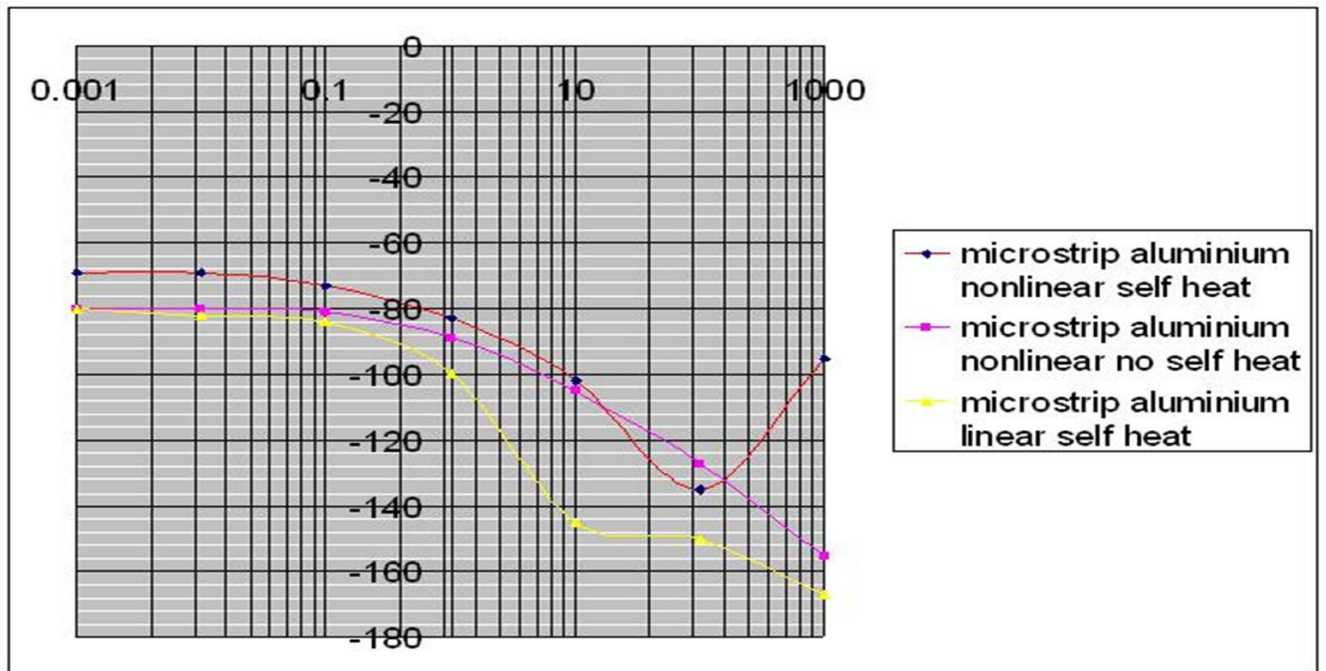


Figure 38 Simplified curve

We can infer the following points from these curves:

1. Self heating does have an impact on IMD as the IMD3 values of aluminium microstrip under varactor induced nonlinearity show a significant increase when self heating is present.
2. Hence self heating is very important.
3. There is a nonlinear region in the curve at high frequencies (around 10 to 1000 MHz). But in this region aluminium microstrip show much better performance than their tantalum counterparts.

## 2.14 SUMMARY

Thus we conclude by stating that we have obtained an equivalent circuit that explains self-heating effects and have tested the presence of nonlinearity and IMD using simulation.

**The significance of the approach lies in successfully modeling thermal effects in interconnects in ICs using SOI technology with Al conductors.**

Future work: proposing of circuits and techniques that can be used for compensation of self-heating effects.

## 2.15 REFERENCES

- [1] R. Wilkerson, K. G. Gard, A. G. Schuchinsky, M. B. Steer, "Electro-thermal theory of intermodulation distortion in lossy microwave components", IEEE Trans. on Microwave Theory and Techniques, vol. 56, no. 12, Part I, pp. 2717-2725, Dec. 2008.
- [2] Eduard Racas et al., "Third Order Intermodulation Distortion due to self heating in Gold Coplanar Waveguides", IEEE Trans. on Microwave Theory, October 2010.
- [3] Jose Pedro and Nuno Carvalho, "Intermodulation Distortion in Microwave and Wireless Circuits", Artech House, 2003.